JOURNAL OF MATERIALS SCIENCE **34** (1999) 3821–3829

Determination of surface heterogeneity by contact angle measurements on glassfibres coated with different sizings

V. WOLFF, A. PERWUELZ, A. EL ACHARI, C. CAZE
Laboratoire de Génie et Matériaux Textiles GEMTEX, Ecole Nationale Supérieure des Arts et Industries Textiles 2, Place des martyrs de la Résitance 59070 Roubaix Cedex 1, France

E. CARLIER
Owens Corning Fiberglas France SA, BP13 L'Ardoise 30290 Laudun, France
E-mail: anne.perwuelz@ensait.fr

This study has been achieved on industrial products (glassfibres coated with different sizings). Contact angle measurements and contact angle hysteresis were obtained with three liquids (glycerol, tricresylphosphate and mineral oil). Fibres are perfectly wetted with tricresylphosphate and mineral oil contrary to glycerol. For this last liquid a large distribution of contact angle and contact angle hysteresis were observed. Three parameters were used to analyse the results: places where filaments were extracted in the roving (inside or at the periphery), roughness and heterogeneity of the filaments surfaces (chemical heterogeneity). Statistical measurements of contact angles have shown heterogeneity in the roving. Atomic force microscopy (AFM) measurements have shown that roughness has only a weak contribution to the large distribution observed on the wetting results with glycerol. This large distribution and the contact angle hysteresis were due to the chemical heterogeneity of the fibres' surfaces.

1. Introduction

Contact angle is a convenient measure of wettability because it is sensitive to the variation of surface properties. A low contact angle (θ) indicates a good wetting. In an ideal gas-liquid-solid system, where the solid is smooth, homogeneous planar and nondeformable, the contact angle θ is related to the surface tension and to the interfacial energies by the Young's equation 1 [1]:

$$\cos\theta_o = (\gamma_{sg} - \gamma_{sl})/\gamma_{lg} \quad (1)$$

where θ_o is the Young's angle or the intrinsic contact angle, γ_{sg} is the surface energy of the solid in the presence of the vapour of the liquid, γ_{lg} is the surface tension of the liquid and γ_{sl} is the interfacial solid-liquid energy. With those parameters, the spreading coefficient S was defined:

$$S = \gamma_{sg} - \gamma_{sl} - \gamma_{lg} \quad (2)$$

and if $S > 0$, the wetting is complete.

Most of the surfaces are not ideal: two parameters are important with regard to contact angle: roughness and compositional heterogeneity of the surface. The influence of these two parameters is reported in Equation 3 [2] and Equation 4 [3]:

$$\cos\theta_W = r \cdot \cos\theta_o \quad (3)$$

θ_W is Wenzel's angle, θ_o is the intrinsic contact angle and r is the roughness factor (ratio of the real to the geometric surfaces).

$$\cos\theta_C = f_1 \cdot \cos\theta_{o1} + f_2 \cdot \cos\theta_{o2} \quad (4)$$

θ_C is Cassie's angle, θ_{o1} and θ_{o2} are the intrinsic angle of two types of regions where f_1 and f_2 are the fractions of each surface area. θ_W and θ_C are angles in equilibrium state.

Moreover, the effect of roughness or compositional heterogeneity cannot be expressed simply in terms of an increase in the solid area or a mixture law because Equations 3 and 4 do not suggest the existence of two experimental contact angles θ_a and θ_r ($\theta_a > \theta_o > \theta_r$) respectively obtained when the triple line advances and recedes, and it is the difference between these two angles which determines the width of contact angle hysteresis.

Different authors have studied these two types of contact angle in considering the wetting of liquid on a solid surface with regular roughness or heterogeneity [4–7]. All these models give a potential curve for each contact angle. This curve shows the existence of numerous metastable states separated by energy barriers between adjacent states. The absolute minimum occurs at the Wenzel's or Cassie's angle (stable equilibrium); the energy barriers are higher nearer Wenzel's or Cassie's angle, and approach zero at the maximum advancing and the minimum receding angle. So, on an "imperfect" surface, according to the speed and the liquid motion

direction on the solid surface, the appearent angle can take all the possible values in metastable equilibrium. The values θ_o, θ_a, θ_r are difficult to accede in experiments [8]. They depend on the jumping of triple line over the energy barriers which are themselves due to topographic defects [9–11] or chemical heterogeneity of surfaces [12–16].

More recently, Joanny and DeGennes [17] developed a theoretical approach with a random distribution of defects, which are closer to reality. The equilibrium position of triple line results in an equilibrium of the force of the defect and the restoring force. Di Méglio and Quéré [18] tried to relate random roughness to contact angle hysteresis but experiments on random rough surfaces are difficult to interpret. Indeed authors do not know which or how many of roughness parameters are to be chosen to take into account the real distribution of size and position of the topological defects.

The aim of this work was to study industrial surfaces: fibreglass coated with different sizings. Organosilanes coupling agents are widely used as primers on glassfibres to promote the adhesion between the resin and the glass in fibreglass reinforced polymer [19]. Industrially, instead of depositing the coupling agent only, a mixture known as sizing (composed of: a film former, a lubricant, some additives and a coupling agent) is used. Contact angle measurements were used to characterize fibres having been coated on the one hand with a complete sizing treatment and on the other hand to a coupling agent treatment only. Variation of contact angle along the fibre and contact angle hysteresis were studied. The results thus obtained, were then discussed in terms of surface heterogeneity which was also investigated by atomic force microscopy (AFM). These two techniques (contact angle and AFM) are very surface sensitive and their comparison is of particular interest [20], since there is only little experimental evidence of the relation that may exist between the local structure (as can be probed by AFM) and the macroscopic contact angles.

2. Experimental

2.1. Materials

2.1.1. Fibres

E-glass fibre were manufactured in the form of rovings by Owens Corning Fiberglass. Each roving contained 800 filaments (each filament having a round cross-section and a diameter of 14 μm).

The glassfibres were coated with four different kinds of sizing: two sizings contained each, a coupling agent only (A1100: γ-aminopropyltriethoxysilane or A187: γ-glycidoxypropyltrimethoxysilane) and the other two were complete sizings each containing a film former, a lubricant, additives and a coupling agent (A1100 or A187).

Table I shows the name given to the sizing glass fibres.

TABLE I Name of the glassfibres tested

	Name
Coupling agent A1100	A1100
Coupling agent A187	A187
Sizing with coupling agent A1100	SA1100
Sizing with coupling agent A187	SA187

2.1.2. Liquids

Three liquids were used for the contact angle measurements, a polar one: glycerol and two non-polar ones: tricresylphosphate and mineral oil. Table II gives the characteristics of these two liquids [21].

TABLE II Characteristics of liquids used for the contact angle measurements

	γ_1 (mJ·m^{-2})	γ_1^D (mJ·m^{-2})	γ_1^P (mJ·m^{-2})
Glycerol	63.4	37.0	26.4
Tricresylphosphate	40.9	39.2	1.7
Mineral oil	30.2	30.2	0.0

We verify the influence of the contact of liquids with the four types of glassfibres, on the surface tension of the wetting liquids (using a Prolabo TD2000 tensometer). In a beaker, a fixed volume of glycerol, 1/15 of its corresponding volume of glassfibres were mixed. This proportion represents the mean value of the droplet volume on a wetted fibre. The beaker was then allowed to stand for 30 min (the time normally needed to measure contact angles all along a filament).

2.2. Methods

2.2.1. Contact angle measurement

The measurement of contact angle between a liquid and a plane solid surface to quantify wettability is a well-known technique [8]. Corresponding measurements of the contact angle between a microdroplet and a monofilament is not easy. The direct tangent method is difficult, as the radius of curvature of the liquid meniscus at the three-phase boundary is quite small (of the order of fibre radius) and a tangent line is nearly impossible to be drawn [8]. Contact angles on filaments have also been measured by the drop profile method [22, 23].

Pressure difference between liquid phase and gas phase (ΔP) is given by Laplace equation:

$$\Delta P = \gamma_{lv}\,(1/R_1 + 1/R_2) \tag{5}$$

where γ_{lv} is the surface tension between liquid and gas, and $1/R_1$ and $1/R_2$ are normal curvatures of the surface whose curves on the surface are perpendicular to each other.

In the case of a droplet on a monofilament (Fig. 1):

R_1: radius of curvature of curve $y = f(x)$ (= distance from drop surface to x-axis)

$$R_1 = -[1 + (\mathrm{d}x/\mathrm{d}y)^2]^{3/2} \big/ (\mathrm{d}^2y/\mathrm{d}x^2) \tag{6}$$

R_2: represented as a function of x and y gives:

$$R_2 = y[1 + (\mathrm{d}y/\mathrm{d}x)^2]^{1/2} \tag{7}$$

In our laboratory, contact angle are calculated by a computer program having been elaborated by Flambart [24] who used equations developed by Yamaki and Katayama [22].

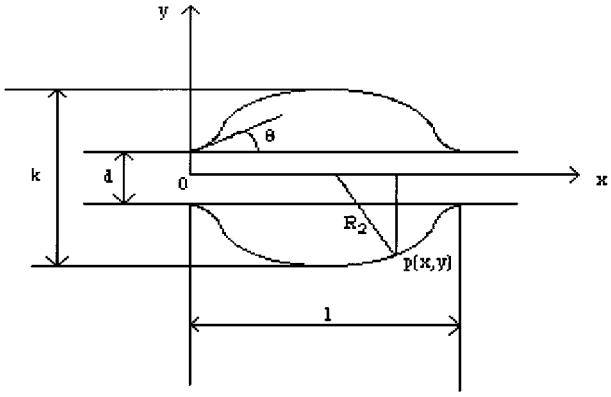

Figure 1 Droplet on a monofilament.

Thus, by measuring l, k and d (where $l =$ length of a droplet, $k =$ height of the droplet and $d =$ diameter of the filament) (Fig. 1), the contact angle can be obtained by the computer program. In the program, d, l and k were used to calculate $K = k/d$ and $L = 2l/d$ so that the diameter become unitary. The program set arbitrary a C constant and a tan θ value. A first dichotomy reaches a value near to L by variation of C. The K deduced from the L calculated is compared to the real K of the droplet. The tan θ value is then changed in order to come closer to the real value of K by the means of a second dichotomy. These both operations were repeated until the calculated K and L are close to the droplet's dimensions.

The error in contact angle is determined. In general, the error is approximately 1° but depends on the drop size [24].

Each E-glass roving being composed of 800 filaments, one filament was extracted and then glued onto a "U" support. Precautions were taken so as not to contaminate the filament (with the fingers for example). A liquid drop was on the filament for the measurement of the contact angles.

For each roving, ten filaments were extracted and on each filament, ten different measurements were made.

The dimensions of each droplet were measured by an apparatus composed of a light microscope (×20), a camera (I2S, IVC800B/C) and a computer (PC compatible) with the PCSCOPE software.

2.2.2. Atomic force microscopy [25] (AFM)

Atomic force microscopy experiments were made, following the procedure established in our laboratory for fibre observation [25]. The AFM measurements were achieved in the air under atmospheric pressure with a commercial scanning probe "Nanoscope III" microscope (Digital Instruments Inc.).

The constant spring of the cantilever was $k =$ 0.06 N/m. The forces used were typically in the range of (1–5)10^{-8} N, and they varied according to the nature of the fibre in order not to damage the surface.

For each image, it is possible to calculate the mean roughness (R_a) of the fibre in the region concerned. Mean Roughness (R_a) is the mean value of the surface relative to the centre plane and is calculated using:

$$R_a = (1/L_x L_y) \iint_{L_x L_y} f(x, y)\, dx\, dy \qquad (8)$$

where $f(x, y)$ is the surface relative to the centre plane and L_x and L_y are the dimensions of the surface.

2.2.3. Scanning electron microscopy (SEM)

The scanning electron micrographs were taken with a STEM JEOL ASID 4-D. Gold coating of the samples was carried out using a BALZERS UNION SCD 040 vacuum coating unit, run at 25 mA for 2 min to obtain a sufficient thick layer without heating the specimen.

3. Results

3.1. Mineral oil and tricresylphosphate

With the two liquids, contact angles for each fibre are weak or near zero. In spite of the observation of non-spread droplets, fibres can be considered as completely wetted [26, 27].

DiMeglio [28] showed how to verify this phenomenon of the instability of Rayleigh. We only need to observe a small droplet emptying its contents into a neighbouring big droplet. This phenomenon is described as "phagocytage" of a small drop by a large drop which is named "cannibal droplet".

According to Laplace, we know that the pressure inside a little droplet is more important than the pressure inside a big one. If the liquid completely wets the fibre, a microscopic film is formed between the two droplets. And the little droplet merges into the big one to minimizise the system's energy. As the phenomenon's kinetic is slow: 12 or 24 h, the liquid used is not volatile.

This experiment was realized with all fibres with TCP and mineral oil. And we can conclude that fibres are completely wetted by these liquids. Hence, fibres have $\gamma_s^d > 40$ mJ·m^{-2} (γ_l^d of TCP).

3.2. Glycerol

A1100 fibre was completely wetted with glycerol. This point will be considered later in the discussion.

Fig. 2 shows the variation of contact angle along three different filaments of A187 fibre. The distribution of contact angle for each filament is wide: 30–35° in one filament. There is heterogeneity on filament. If we compare filaments, filament ♦ has a distribution ranging

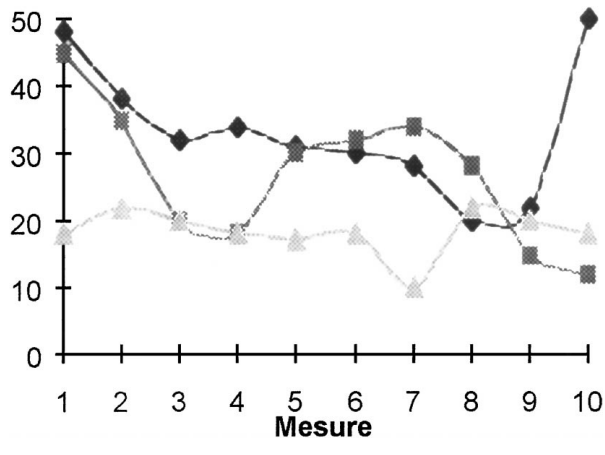

Figure 2 Variation of contact angle along filament wetting liquid: glycerol, fibre: A187.

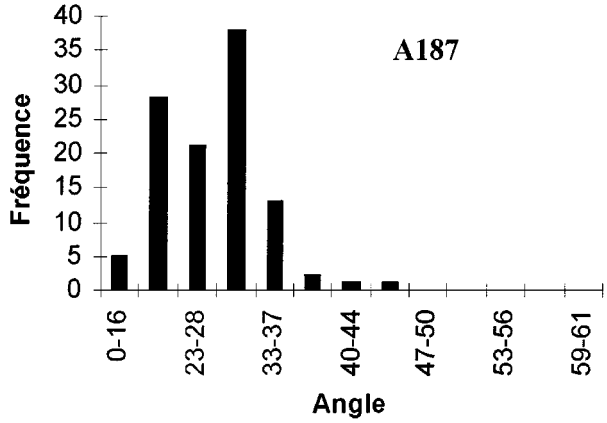

Figure 3 Receding contact angle histogram with glycerol for A187.

from 30° to 40° and filament ▲ has a distribution ranging from 15° to 20°. This shows heterogeneity among filaments too.

This variation is so important that it is impossible to give a precise mean value for an average of the contact angle and we opted for a histogram representation of the results. Fig. 3 represents the frequency of measured angles for each angle distribution range. These ranges were not proportional (0–16° or 59–61°) because they are determined with cos θ a non linear function (function of the contact angle program). These ranges were proportional to cos θ but for an easy reading the histograms were represented in function of angle.

If the angle distributions are looked at more closely, two different distribution can be noticed. With Fig. 2, the filament ▲ belongs to the first distribution (low angles) and the filaments ■ or ♦ belong to the second distribution (large angles). Figs 4 and 5 represent respectively the distribution in receding and in advancing angle. Figs 6 and 7 represent the frequency of measured receding angle distribution for SA1100 and SA187. Figs 8 and 9 represent the frequency of measured advancing angle distribution for SA1100 and SA187.

The mean contact angle values of each distribution are reported in the Table III (1: first distribution, 2: second distribution). We have determine the variation of contact angles ($\Delta\theta$) for each distribution (difference between the higher range and the lower range) in Table IV. Table V summarizes the calculated wetting hysteresis.

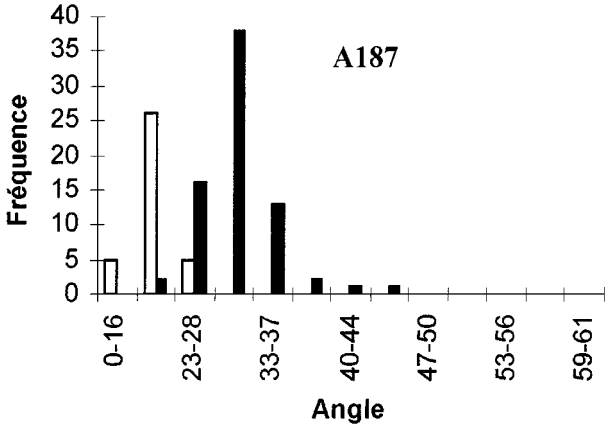

Figure 4 Receding angle distribution with glycerol for A187.

TABLE III Advancing and receding contact angle with glycerol

	θ_{a1}	θ_{a2}	θ_{r1}	θ_{r2}
A187c	26.2 ± 2.4	18.7 ± 3.8	18.7 ± 3.8	31.6 ± 4.4
EA1100	38.1 ± 3.6	55.7 ± 5.9	31.6 ± 3.6	40.2 ± 2.7
EA187	46.0 ± 2.0	54.2 ± 1.5	45.9 ± 2.4	54.0 ± 2.3

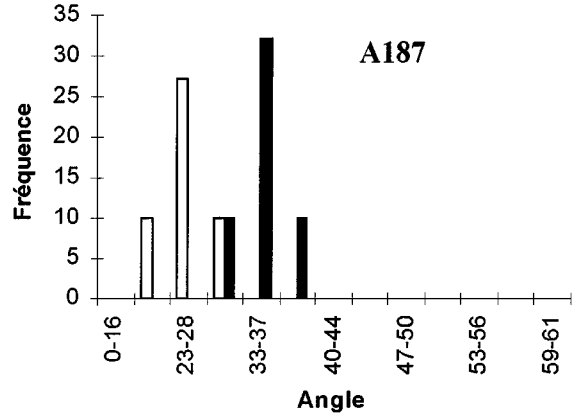

Figure 5 Advancing angle distribution with glycerol for A187.

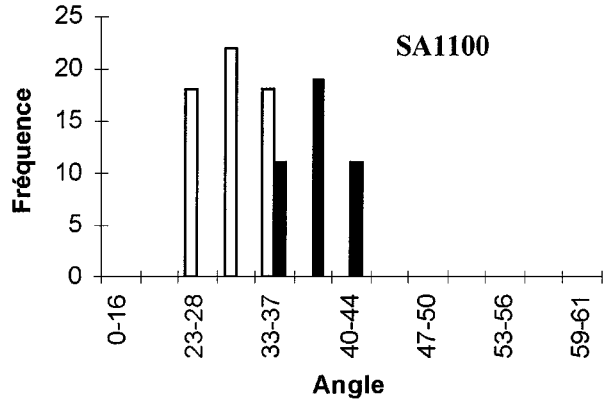

Figure 6 Receding angle distribution with glycerol for SA1100.

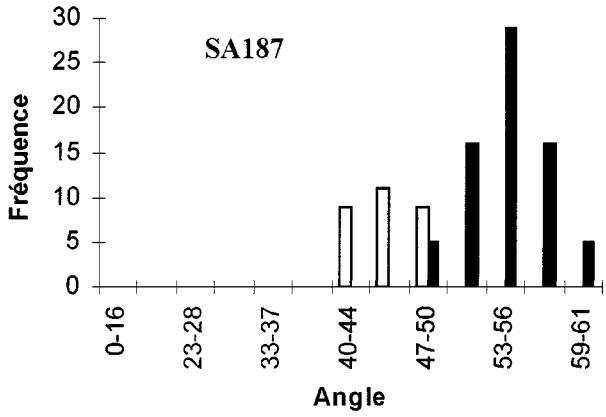

Figure 7 Receding angle distribution with glycerol for SA187.

4. Discussion

Studies on wettability generally show that surface contact angle varies with the roughness and/or with the chemical composition of a surface [29–32]. Recently, Tagawa *et al.* [33] studied the local deviation in contact angles on a single fibre by the weight trace for the fibre with the Wilhelmy technique and discussed the

TABLE IV The angle variation of different fibres

	$\Delta\theta_{a1}$	$\Delta\theta_{a2}$	$\Delta\theta_{r1}$	$\Delta\theta_{r2}$
A187c	17°	12°	28°	31°
EA1100	15°	20°	15°	10°
EA187	10°	10°	15°	15°

TABLE V Hysteresis values

	H_1	H_2
A187	7.5	4.0
SA1100	6.5	15.5

$H_1 = \theta_{a1} - \theta_{r1}$
$H_2 = \theta_{a2} - \theta_{r2}$

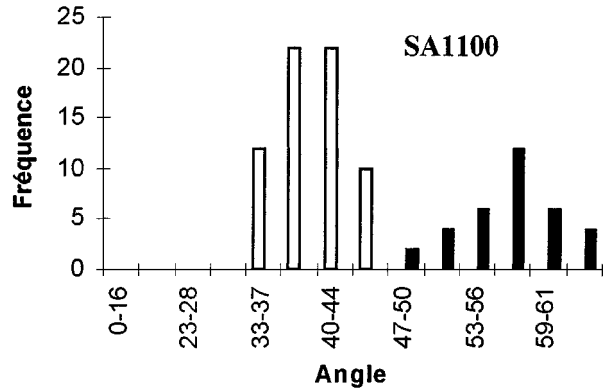

Figure 8 Advancing angle distribution with glycerol for SA1100.

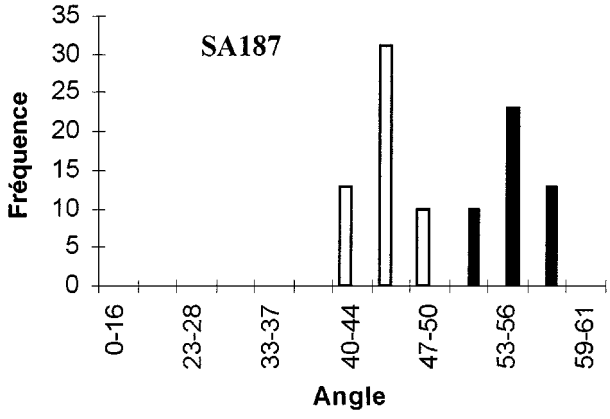

Figure 9 Advancing angle distribution with glycerol for SA187.

variation in terms of surface heterogeneity. The deviation of the advancing and receding angles for our fibres with different liquids was studied by the spreading drop technique.

4.1. A1100 fibre

As the fibre A1100 was perfectly wetted by glycerol, the A1100 should have a high surface energy according to Equation 2 but this is inconsistent with the values found in the literature: Wu [8] (35.7 mJ/m^2) and Plueddemann [19] (34.2 and 42.8 mJ/m^2). The silane/glass link was a hydrogen bond or covalent one. The ideal mechanism with monomoleculary layer can't be found in the reality. Ishida and Koening [34] showed that with FTIR techniques. Wang *et al.* [35, 36] studied by TOFSIMS and XPS these interaction of silane/glass. A gradient of polymerization in coupling agent has been detected in the physisorbed polysiloxane layers. Chabert *et al.* [37] have showed that the first layers of A1100 are chemically attached to the fibre; other few layers (∼10) are chemisorbed polysiloxanes and the last hundred layers, principally monomers and oligomers, are physically adsorbed silane hydrolyzates which are rapidly removed by cold water rinse. The pictures obtained by the atomic force microscopy [25] show that in the case of A1100, the distribution of the coupling agent on the fibre was done in the form of droplets; there is formation of "islands" on the fibre. Many authors [37, 38] say that between the "islands" a single layer of coupling agent occurs. The coupling agent deposited on the fibre was present in a very large quantity (0.2% weight/fibre). So, islands which had quite important dimensions (0.02 μm high for a diameter of 0.6 μm) [25] represented molecules which were physically adsorbed. We think that these physically adsorbed molecules would be removed by the glycerol. And we confirm this hypothesis by measurements of surface tension of glycerol in which A1100 fibres had been soaked. Thirty minutes after the immersion of fibres, the surface tension of glycerol fell from 64.4 mJ/m^2 to 55.0 ± 4 mJ/m^2.

The contact of fibre A1100 with glycerol may induce the variation of fibre's surface energy and at the same time the decrease of glycerol's surface tension. A1100 fibre looks perfectly wetted not because of its high surface energy but more probably because of these exchanges between solid and liquid.

4.2. A187, SA1100 and SA187 fibres

With glycerol, contact angle distributions were wider (Figs 4–9). The results obtained by the analysis of the contact angle variation (Table IV) and by the calculation of hysteresis (Table V) could be interpreted in terms of chemical or physical heterogeneities. By heterogeneities, it is meant that there is a non-wetting surface which contains less or more wettable defects.

As far as the physical aspect is concerned, the heterogeneity is due to the roughness of surfaces. The chemical aspect concerns the chemical heterogeneity of the surface. Another cause of chemical hysteresis is the transport of molecules to the liquid across the solid surface. We have verified that the surface tension of glycerol does not change during the experiment. And the last major cause of chemical hysteresis, with certain polar solids, is the reorientation of molecules or groups [39, 40] in the solid surface under the influence of the liquid phase. This last phenomenon was eliminated from our interpretation. As the sizings were reticulated 11 h at 115 °C, the sizings' T_g was supposed to be superior to the room temperature.

Actually, the variation of contact angle and its hysteresis give more information about the fibre's surface: the one giving a more microscopical approach and the other one a more macroscopical vision of the surface. All the same, these two can be linked to each other as we will see later in this paper.

As a matter of fact, it is easily understandable that if the surface consists of uniformly distributed heterogeneities, there won't be any variation of contact angle, but there would nevertheless be contact angle hysteresis (as it was noted by Tagawa *et al*. [33]). Instead, if the heterogeneities are non uniformly distributed the contact angle will fluctuate and there will be wetting hysteresis.

4.2.1. A187 fibre

We have seen two different distributions on our histograms. These double distributions don't represent two kinds of heterogeneities but two kinds of filaments. This result could be explained by the fact that during the passage through the sizing bath, filaments are not impregnated in the same way by the sizing bath. The filaments get at 500–1000 m/min tangential speed over a roller which turn at 20–25 tr/min in the sizing bath. In fact, filaments were not impregnated one-to-one but on 200 filaments packet. It can be thought that the two types of filaments each having different heterogeneities are representatives of filaments inside and outside of the roving. This was confirmed by the AFM technique. Figs 10 and 11 represent a filament outside and inside respectively.

Inner filaments are glued together by the coupling agent and when they are pulled out of the roving their surface have patches of higher energy. The first distribution correspond to inner filaments. The outer filaments have more risk to be polluted and so that have a lower surface energy. So, on Figs 4–7, the first distribution represented inner filaments and the second outer filaments.

On Table III, we could see that for both distribution the standard deviation in receding contact angle was higher than the standard deviation in advancing contact angle. The variation of the contact angle could be due to roughness or due to chemical composition.

Let us now interpret the nature of heterogeneities. Contact angle variation as far as the physical heterogeneities are concerned is due to the topographic variation of the surface. AFM measurements [25] allow us to visualize the topography of our fibres. Their surface is globally smooth and this was confirmed by the measurement of R_a [25] by AFM. Eick and Good [5] showed that there is no hysteresis when the characteristic dimensions of the roughness fall below about 0.1 μm.

So the angle distributions of our fibres are due to chemical composition variation of the surface. With AFM measurement we showed heterogeneous surfaces [25]. In fact, filaments are glued together by the coupling agent (Fig. 12). When a filament is pulled out from its neighbouring filaments, a tearing was created. In this tearing, density could be different in fact there are

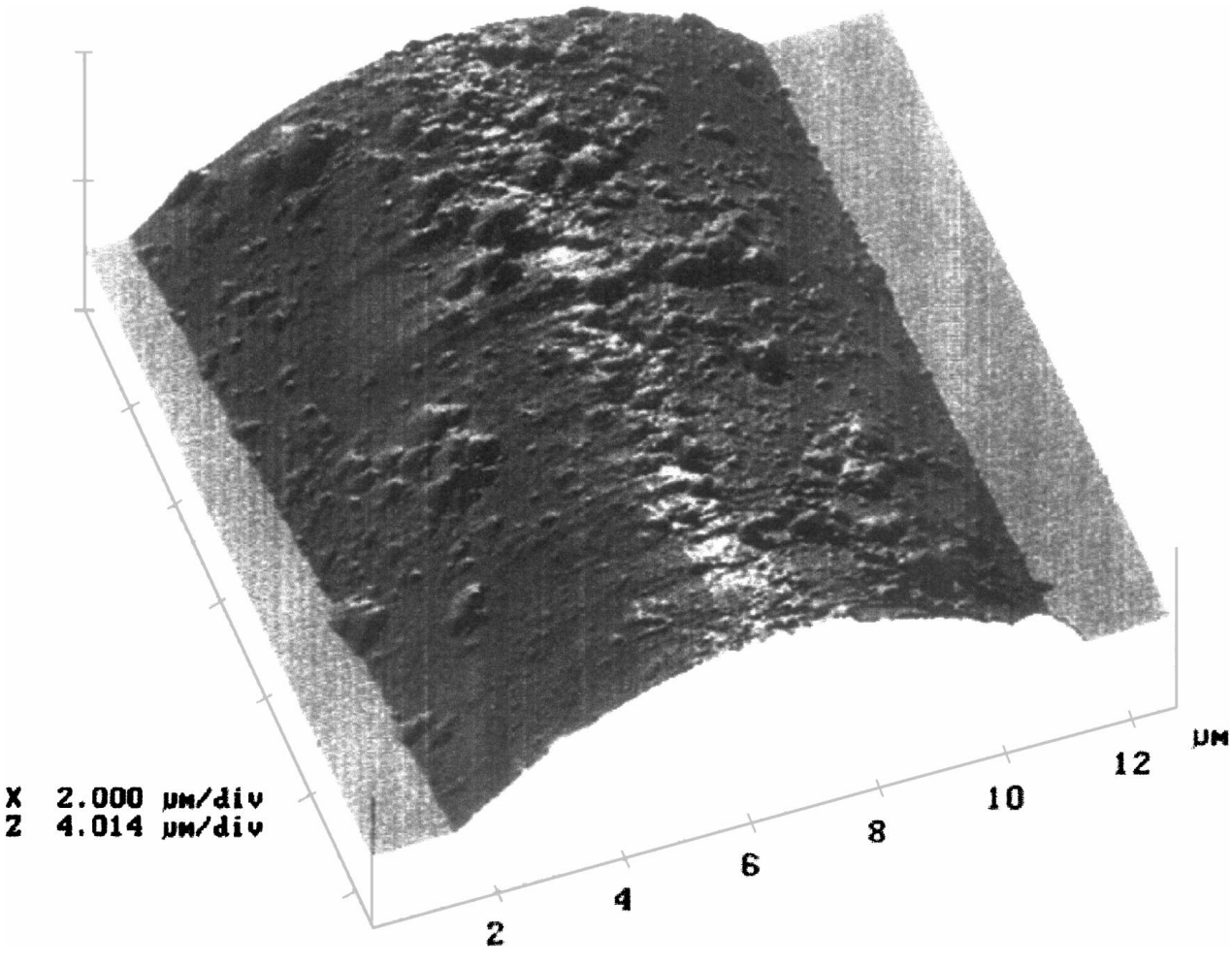

Figure 10 AFM image of the A187 fibre outside of the roving.

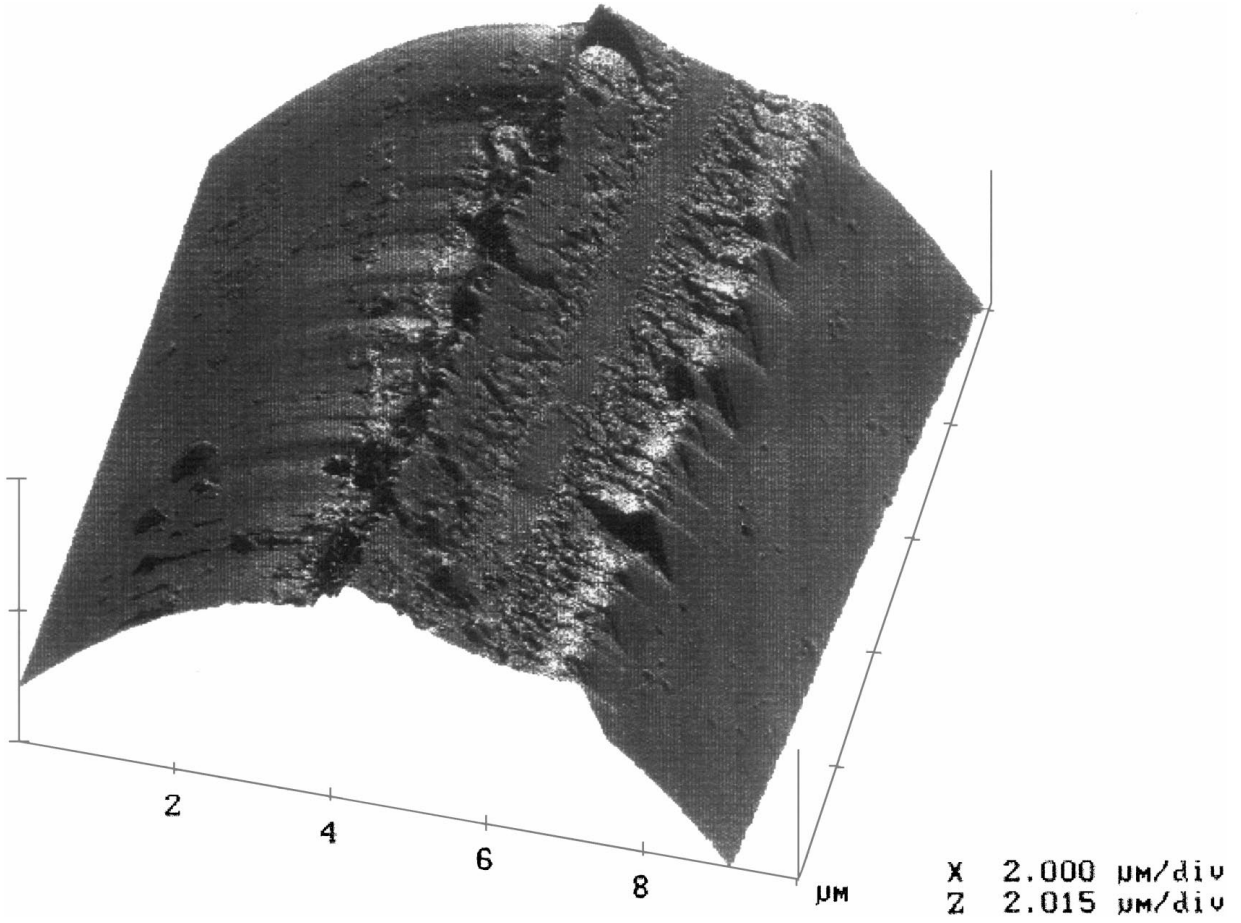

Figure 11 AFM image of the A187 fibre inside of the roving.

different degrees of polymerisation in coupling agent layers [35, 36]. The geometric effect of the tearing in form of drain played a part too. These effects explain the contact angle variation.

Johnson and Dettre [6] have shown that receding angles are more sensitive to fractional coverages by high-energy on predominantly low-energy surfaces whereas advancing angles are more sensitive to fractional coverages by low-energy region on predominantly high energy surfaces. Table IV summarizes the variation of contact angle ($\Delta\theta$) of the different distributions. For this fibre, for each distribution $\Delta\theta_a < \Delta\theta_r$, the surface have defects of higher surface energy.

4.2.2. SA1100 and SA187 fibres

Well, if we just try to see more closely the difference between the wetting behaviour of a fibre covered by coupling agent only, and that of a fibre having been submitted to a complete sizing treatment, (e.g., the A187 and the SA187) we will see that the coupling agent is better wetted than the complete sizing, and this is true for the A1100, too. In the sizing (SA1100 and SA187) there is a lubricant which aims at separating filament from each others and the non-wetting character of lubricants is well known.

Considering the complete sizing: SA1100 and SA187 which have confidential compositions, nevertheless it is possible to affirm that the film former which is the main constituent is going to cover completely the fibre [25]. The contact angle variation (Table III) is due to the distribution of the different constituents: lubricants, additives, coupling agent and a film former which are going to organize among themselves to form a blend of a composite surface.

We have determined the variation of contact angle ($\Delta\theta$) of each distribution (Table IV). For the second distribution for SA1100, $\Delta\theta_r < \Delta\theta_a$. We are in the case of a predominantly high-energy surface with low-energy defects [6].

Let's look at wetting hysteresis (Table V). For the SA187, whatever are the distributions, wetting hysteresis can't be detected and the contact angle variations are small. Distribution of film former and additives is homogeneous.

For the SA1100, the same argument as for A187 fibre can be used to point out the distribution corresponding to inner filaments and the one corresponding to outer ones. The first distribution represents inner filaments as they are "protected" from the external environment. The other filaments are easily polluted and have thus their surface energies decreased. Otherwise, we can consider that the outer filaments are going to organize so as to decrease their surface energy according to atmosphere while the surface energy of the inner fibres is going to obtain equilibrium within internal environment. We can note that the hysteresis values (Table V) are different according to the distributions. These values are more considerable on outer filaments. Hence, not only is there the absence of a uniform penetration of the film former,

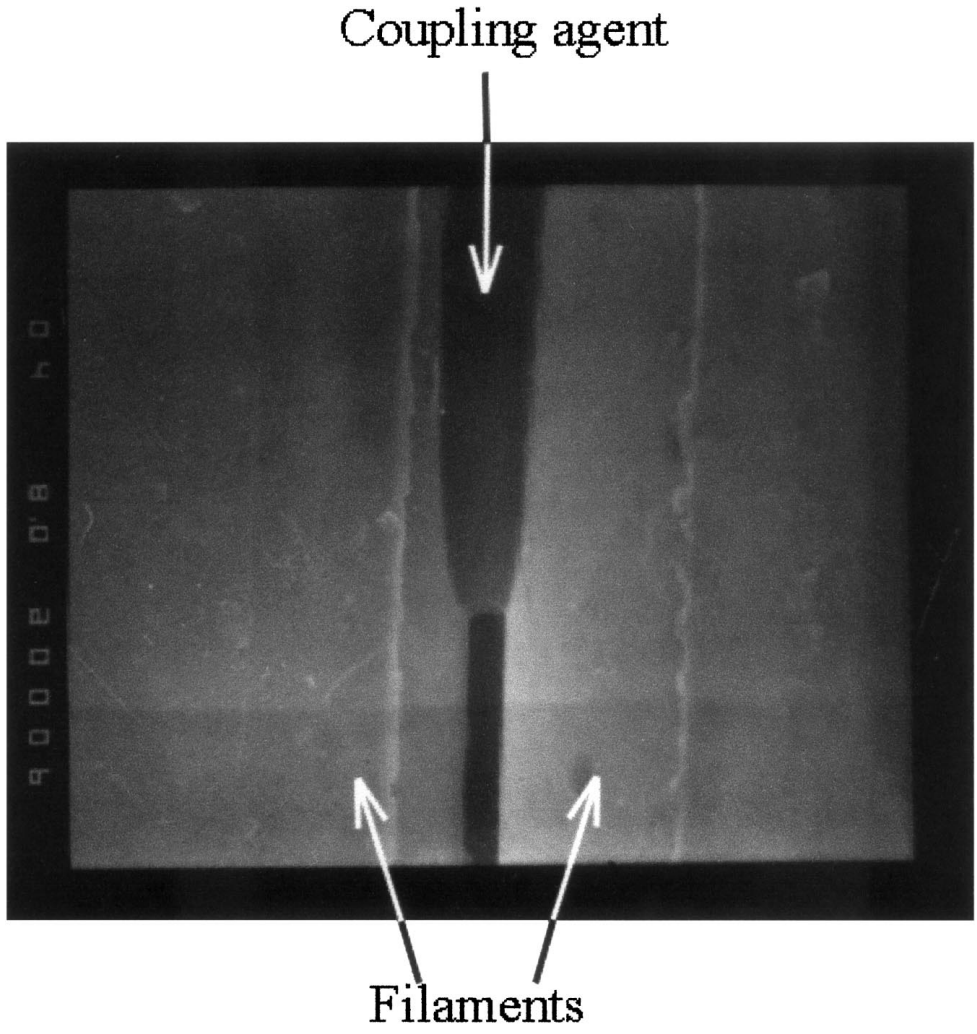

Figure 12 SEM image of the A187 fibre: two filaments glued by the coupling agent.

but furthermore the additives and lubricants don't flow in the same way in the inner and outer part of the roving.

5. Conclusion

Wettability of glassfibres is a fundamental characteristics particularly when these have to be coated with a resin.

Contact angle measurements on industrials fibreglass filaments were performed by using three different liquids, and the results thus obtained allowed not only to forecast the wettability of fibres but also revealed local heterogeneities on the fibres' surface.

The four types of glassfibres were totally wetted with non-polar liquids: mineral oil and TCP (having a surface tension lower than 40 mJ/m^2), and Rayleigh's instability was observed.

With the polar liquid: glycerol, only the A1100 fibre was totally wetted. The other three fibres showed each, a large contact distribution range which was principally due to chemical heterogeneities.

We showed that all the filaments of a same roving do not have the same surface composition (or structure). They can be classified into two families: outer filaments and inner filaments. The inner filaments have always a higher surface energy.

These heterogeneities were quantified either by the wideness of the distribution range of the advancing or of the receding angles or by the hysteresis value: in any case the result was the same. Whatever is the coupling agent used, with both complete sizing we obtain a smooth fibre surface. However, in one case the chemical composition is homogeneous and in the other one it is heterogeneous with low energy defects.

Although the coupling agent was not the unique component of the sizing used on the fibre's surface, its chemical nature played a part in the sizing organisation inner or outer the roving.

Acknowledgements

We should like to express our gratitude to N. Behary, T. Novais de Olivera and X. Flambart for the measurements and calculation of contact angles and L. Brunet for the measurements by SEM.

References

1. T. YOUNG, *Trans. R. Soc. London* **95** (1805) 65.
2. R. N. WENZEL, *Industrial and Engineering Chemistry* **28**(8) (1936) 988–994.
3. A. B. D. CASSIE, *Discuss. Faraday Soc.* **3** (1948) 11–16.
4. R. J. GOOD, *J. Amer. Chem. Soc.* **74** (1952) 5041–5042.
5. J. D. EICK, R. J. GOOD and A. W. NEUMANN, *J. Colloid and Interface Sci.* **53**(2) (1975) 235–248.
6. R. E. JOHNSON JR. and R. H. DETTRE, *J. Phys. Chem.* **68**(7) (1964) 1744–1750.

7. A. W. NEUMANN and R. J. GOOD, *J. Colloid and Interface Sci.* **38**(2) (1972) 341–358.
8. S. WU, "Polymer Interface and Adhesion" (Marcel Dekker, New York, 1982).
9. A. W. NEUMANN, D. RENZOW, H. REUMUTH and I. E. RICHTER, *Fortschr. Koll. Polym.* **55** (1971) 49.
10. V. DEJONGHE, D. CHATAIN, I. RIVOLLET and N. EUSTATHOPOULOS, *Journal de Chimie Physique* **87** (1990) 1623.
11. V. DEJONGHE and D. CHATAIN, *Annales de Chimie Françaises* **15** (1990) 485.
12. J. KONAR, A. K. SEN and A. K. BHOWMICK, *J. Appl. Poly. Sci.* **48** (1993) 1579.
13. R. E. JOHNSON Jr, R. H. DETTRE and D. A. BRANDRETH, *J. Colloid Interface Sci.* **62** (1977) 205.
14. Y. L. CHEN, C. A. HELM and J. N. ISRAELACHVILI, *J. Phys. Chem.* **95** (1991) 10736.
15. J. RAULT, A. AOUINTI, M. GOLDMAN and A. GOLDMAN, *Compte Rendue de l'Académie des Sciences Paris II* **309** (1989) 333.
16. M. E. R. SHANAHAN, A. CARRE, S. MOLL and J. SCHULTZ, *Journal de Chimie Physique* **83** (1986) 351–354.
17. J. F. JOANNY and P. G. DEGENNES, *Journal of Chemie and Physics* **81** (1984) 552–562.
18. J. M. DI MÉGLIO and D. QUÉRÉ, *Europhysics Letters* **11** (1990) 163.
19. E. P. PLUEDDEMANN, "Silane Coupling Agents" (Plenum Press, New York, 1982).
20. A. BARRAT, P. SILBERZAN, L. BOURDIEU and D. CHATENAY, *Journal de Chimie Physique* **20** (1992) 633.
21. J. BRIANT, "Phénomènes d'interface Agents de Surface" (Editions Technip, Paris, 1989).
22. J. I. YAMAKI and Y. KATAYAMA, *J. Appl. Polym. Sci.* **9** (1975) 2897–2909.
23. B. J. CARROLL, *J. Colloid and Interface Sci.* **57**(3) (1976) 488–495.
24. X. FLAMBART, Rapport de DEA, GEMTEX-ENSAIT, 1993.
25. A. EL ACHARI, A. GHENAIM, C. CAZE, V. WOLFF and E. CARLIER, *Textile Research Journal* **66**(8) (1996) 483–490.
26. F. BROCHARDS, *Journal of Chemie and Physics* **84**(8) (1986) 4664–4672.
27. *Idem.*, *Compte Rendue de l'Académie des Sciences Paris II* **303** (1986) 1077.
28. J. M. DIMEGLIO, *ibid.* **303**(6) (1986) 437–439.
29. F. E. BARTELL and J. W. SHEPARD, *J. Phys. Chem.* **57** (1953) 211, 455, 458.
30. Y. TAMAI and K. ARATANI, *ibid.* **76** (1972) 3267.
31. R. H. DETTRE and R. E. JONHSON Jr., *ibid.* **69** (1965) 1507.
32. B. R. RAY, J. R. ANDERSON and J. J. SCHOLZ, *ibid.* **62** (1958) 1220.
33. M. TAGAWA, A. YASUKAWA, K. GOTOH, N. OHMAE and M. UMENO, *Journal of Adhesion Science and Technology* **6** (1992) 763.
34. H. ISHIDA and J. L. KOENING, *J. Colloid Interface Sci.* **64**(3) (1978) 565–576.
35. D. WANG, F. R. JONES and P. DENISON, *J. Mater. Sci.* **27** (1992) 36–48.
36. *Idem.*, "*Silanes and Other Coupling Agents*," edited by K. L. Mittal (1992) pp. 345–364.
37. B. CHABERT, J. CHAUCHARD, M. ESCOUBES, P. JEANNE and T. M. LAM, *Bulletin de la Société Chimique de France* **1** (1986) 11–16.
38. W. D. BASOM, *Macromolecules* **5** (1972) 792.
39. H. YASUDA and A. K. SHARMA, *J. Polym. Sci.* **19** (1981) 1285.
40. C. VERGELATI, A. PERWUELZ, L. VOVELLE, M. A. ROMERO and Y. HOLL, *Polymer* **35**(2) (1994) 262–269.

Received 8 July 1997
and accepted 17 February 1999